

Contents lists available at ScienceDirect

Journal of Advanced Research

journal homepage: www.elsevier.com/locate/jare



Irisin alleviates obesity-induced bone loss by inhibiting interleukin 6 expression via TLR4/MyD88/NF-κB axis in adipocytes



Yuanshu Zhang ^{a,b,1}, Xu He ^{b,1}, Kai Wang ^{a,b,1}, Yuan Xue ^a, Sihan Hu ^a, Yesheng Jin ^{a,b}, Guoqing Zhu ^c, Qin Shi ^{b,*}, Yongjun Rui ^{a,*}

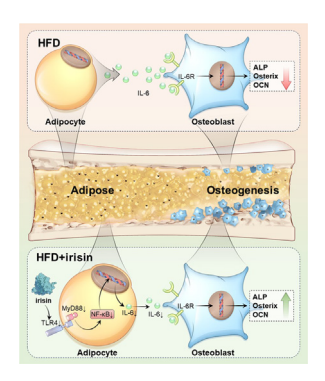
- ^a Department of Orthopedics, Wuxi Ninth People's Hospital Affiliated to Soochow University, Wuxi, Jiangsu 214026, PR China
- b Department of Orthopedics, The First Affiliated Hospital of Soochow University, Orthopedics Institute of Soochow University, Suzhou, Jiangsu 215006, PR China
- ^c Department of Physiology, Nanjing Medical University, 101 Longmian Avenue, Nanjing, Jiangsu 211166, PR China

HIGHLIGHTS

- Adipocytes under obese conditions inhibit osteogenic differentiation of bone marrow mesenchymal stem cells.
- Irisin (a natural human myokine) alleviates obesity-induced bone loss by inhibiting IL-6 secretion from adipocytes.
- Inhibition of adipocyte IL6 secretion by irisin is mediated by inhibition of the TLR4/MyD88/NF-κB pathway.
- The therapeutic potential of irisin in preventing obesity-induced bone loss is revealed.

GRAPHICAL ABSTRACT

Irisin downregulates TLR4/MyD88/NF- κ B pathway in adipocytes and reduce IL-6 production in the adipocytes, consequently alleviates the inhibition of IL-6 on osteogenesis and rescue obesity-induced bone loss.



ARTICLE INFO

Article history: Received 13 January 2024 Revised 10 April 2024 Accepted 13 April 2024 Available online 16 April 2024

ABSTRACT

Introduction: Obesity-induced bone loss affects the life quality of patients all over the world. Irisin, one of the myokines, plays an essential role in bone and fat metabolism.

Objective: Investigate the effects of irisin on bone metabolism via adipocytes in the bone marrow microenvironment.

Methods: In this study, we fed fibronectin type III domain-containing protein 5 (FNDC5, the precursor protein of irisin) knockout mice (FNDC5^{-/-}) with a high-fat diet (HFD) for 10 weeks. The quality of bone

Abbreviations: IL-6, Interleukin 6; HFD, High-fat diet; BMSCs, Bone marrow mesenchymal stem cells; BMAT, Bone marrow adipose tissue; LPS, Lipopolysaccharides; WT, Wild-type; BMD, Bone mineral density; Tb. Sp, Trabecular separation; Tb. N, Trabecular number; CTX, Carboxyterminal telopeptide; H&E, Hematoxylin and eosin; ALP, Alkaline phosphatase; ARS, Alizarin red S; ORO, Oil Red O; qRT-PCR, Quantitative real-time PCR; IF, Immunofluorescent; DEGs, Differentially expressed genes; MAR, Mineralized deposition rate; SD, Standard diet; Runx2, Runt-associated transcription factor 2; OCN, Osteocalcin; IHC, Immunohistochemical; OD, Optical density; TRAP, Tartrate-resistant acid phosphatase; NC, Nitrocellulose membranes; CM, Conditioned medium; MSCs, Mesenchymal stem cells; ELISA, Enzyme-linked immunosorbent assay; CCK-8, Cell Counting Kit-8; P1NP, Type I procollagen N-terminal propeptide; FNDC5, Fibronectin type III domain-containing protein 5; SMI, Structural model index; Conn. D, Connection density; Tb. Th, Trabecular thickness; BV/TV, Bone volume/tissue volume; SPF, Specific Pathogen Free; GO, Gene ontology; KEGG, Kyoto encyclopedia of genes and genomes; GSEA, Gene Set Enrichment Analysis.

E-mail addresses: shiqin@suda.edu.cn (Q. Shi), ruiyongjun@suda.edu.cn (Y. Rui).

^{*} Corresponding authors.

¹ These authors contributed equally to this work.

Keywords: Irisin Adipocytes IL-6 TLR4/MyD88/NF-κB Osteogenesis mass was assessed by micro-CT analysis, histological staining, and dynamic bone formation. *In vitro*, the lipogenic differentiation of bone marrow mesenchymal stem cells (BMSCs) was assayed by Oil Red O staining, and the osteogenic differentiation was assayed by alkaline phosphatase staining. Meanwhile, the gene expression in the BMSC-differentiated adipocytes by RNA sequence and the involved pathway of irisin were determined by western blot and qRT-PCR were performed.

Results: The FNDC5^{-/-} mice fed with a HFD showed an increased body weight, fat content of the bone marrow and bone, and a decreased bone formation compared with those with a standard diet (SD). *In vitro*, irisin inhibited the differentiation of BMSCs into adipocytes and alleviated the inhibition of osteogenesis derived from BMSCs by the adipocyte supernatant. RNA sequence and blocking experiment showed that irisin reduced the production of interleukin 6 (IL-6) in adipocytes through downregulating the TLR4/MyD88/NF-κB pathway. Immunofluorescence staining of bone marrow further confirmed an increased IL-6 expression in the FNDC5^{-/-} mice fed with HFD compared with those fed with SD, which suffered serious bone loss.

Conclusion: Irisin downregulates activation of the TLR4/MyD88/NF-κB pathway, thereby reducing IL-6 production in adipocytes to enhance the osteogenesis of BMSCs. Thus, the rescue of osteogenesis of BMSCs, initially inhibited by IL-6, is a potential therapeutic target to mitigate obesity-induced osteoporosis.

© 2023 The Authors. Published by Elsevier B.V. on behalf of Cairo University. This is an open access article under the CC BY-NC-ND license (http://creativecommons.org/licenses/by-nc-nd/4.0/).

Introduction

Obesity is a rapidly increasing societal concern, which affects the quality of life of people [1–3]. In 2016, the World Health Organization reported that over 1.9 billion adults were overweight and 650 million were obese. Approximately 56 % of elderly people are estimated to be overweight or obese by 2030. Obesity has severe negative implications on various organs and systems, including asthma, hypertension, hyperlipidemia, and diabetes [4]. Obesity was previously thought to be a safeguarding factor for bones because of the amplification of bone formation after mechanical stimulation [5,6]. However, accumulated evidence suggests that augmented body fat and hyperlipidemia decrease bone density Hu, [7,8] Long-term metabolic disorders caused by obesity can decline bone formation and conversion, consequently increasing the risk of fractures [9,10].

In adults, most of the adipose tissue is white, comprising approximately 85 % of the total adipose tissue. Its primary location is within subcutaneous deposits situated in the abdominal region. Brown adipose tissue, constituting approximately 15 % of the total adipose tissue, is primarily located in visceral fat depots. In the skeletal system, bone marrow adipose tissue (BMAT) accounts for nearly 70 % of the volume of the bone marrow [11]. BMAT is neither white fat nor brown adipose tissue, and bone marrow adipocytes are likely to be heterogeneous [12]. The microenvironmental cues in the bone marrow cavity are composed of adipocytes, mesenchymal stem cells (MSCs), and hematopoietic stem cells, which differentiate into blood cells, immune cells, osteoblasts, osteoclasts, and produce various cytokines [13-16]. The BMAT is an endocrine organ that regulates bone remodeling by secreting adipokines and cytokines, which plays a pivotal role in regulating bone metabolism. Adipocytes can influence osteoblasts, osteoclasts, and hematopoietic cells through paracrine signaling pathways [17]. Excessive obesity is considered a chronic, low-grade inflammatory condition [18]. In obesity, inflammatory cytokines derived from adipocytes can affect normal cells in the bone marrow microenvironment, causing obesity-related bone metabolism disorders, leading to bone loss. For example, bone marrow adipocytes secrete adiponectin and interleukin 6 (IL-6) [19,20], which can exacerbate bone loss by promoting osteoclast differentiation [21-23].

Irisin is a myokine that skeletal muscle cells release subsequent to physical exertion and tailored to the FNDC5 protein

and causes white fat cells to turn brown [24], thereby improving obesity [25]. Mazur-Bialy et al. reported that irisin could delay the activation of inflammatory pathways in adipocytes stimulated by lipopolysaccharides (LPS) by suppressing the secretion of TNF-α, and MCP-1 [26]. Moreover, irisin inhibits liver-based glucose production and promotes the synthesis of glycogen [27]. In a mouse obesity study, upregulation of FNDC5 and irisin improved glucose/lipid metabolic imbalances and accelerated lipolysis [28]. We have previously demonstrated that irisin facilitated the osteogenic differentiation of bone marrow mesenchymal stem cells (BMSCs) by activating the BMP/SMAD signaling pathway through αV integrin receptors [29]. Meanwhile, irisin suppresses Ti-particle-induced RANKL production in osteoblasts derived from MSCs and oxidative stress in osteoclasts [30]. A great deal of data compellingly indicates that irisin assumes a vital role in fat and bone metabolism. Since BMAT plays a crucial role in the bone marrow microenvironment [31], investigating the role of irisin in the mutual regulation of adipose tissue and osteogenesis, along with its underlying mechanisms, is of significant importance.

In this study, we evaluated the role of the irisin gene in the obese FNDC5^{-/-} and wild type (WT) mice of bone mass. A high-fat diet (HFD) led to osteoporosis in the WT mice, and irisin deficiency further exacerbated the decrease in bone mass caused by HFD in the FNDC5^{-/-} mice. Subsequently, we discovered that irisin suppressed the release of the inflammatory cytokine IL-6 in adipocytes via the TLR4/MyD88/NF-κB signaling pathway, thereby enhancing BMSC-derived osteogenesis that is typically hindered by IL-6. This study not merely validated the substantial involvement of irisin in obesity-related osteoporosis but also delved into potential novel mechanisms of bone metabolism. By exploring the effects of irisin on fat and bone metabolism, we provide a new idea for improving obesity-related bone diseases.

Materials and methods

Animal protocol

The global deletion of the FNDC5 gene in C57BL/6 mice (FNDC KO, FNDC5^{-/-}) were kindly presented by Professor Guoqing Zhu of Nanjing Medical University, and the identification was performed (Fig. S1A). The WT and FNDC5^{-/-} mice were housed in a Specific Pathogen Free (SPF) animal facility at the Soochow University

Animal Experimentation Center. We divided the 6-week-old male mice into 4 groups based on the genetic identification and fed the mice with a HFD or a standard diet (SD). All the mice were euthanized after being fed for 10 weeks and samples were collected.

Ethics statement

All experimental protocols were approved by the Animal Care Committee of Soochow University (KS2023032).

Micro-CT scanning and analysis

Following well-established protocols, the lower limbs of mice were scanned using the Skyscan system (Bruker, Belgium) [29]. Bone-related parameters, including bone mineral density (BMD), bone volume/tissue volume (BV/TV), trabecular thickness (Tb. Th), connection density (Conn. D), trabecular separation (Tb. Sp), trabecular number (Tb. N), and structural model index (SMI), were assessed according to the methods outlined in the previous descriptions [32].

Enzyme-linked immunosorbent assay (ELISA)

The the levels of type I procollagen N-terminal propeptide (PINP), type I collagen cross-linked carboxyterminal telopeptide (CTX), and IL-6 in the sera was quantified by ELISA kits (Elabscience, China) according to the manufacturer's instructions [32].

Histochemistry and histomorphometry

Femurs were prepared as paraffin or frozen sections, and stained with hematoxylin and eosin (H&E) staining, tartrateresistant acid phosphatase (TRAP) staining (Sigma Aldrich, USA) to detect osteoclasts, and Masson staining (Salorbio, China), respectively. The expression of runt-associated transcription factor 2 (Runx2), Osterix, and osteocalcin (OCN) was analyzed by immunohistochemistry of frozen sections (Abcam, USA, Supplementary Table 2).

Dynamic bone formation

The configured calcein solution (5 mg/ml, 15 mg/kg body weight, Sigma, USA) was injected intraperitoneal into each mouse on days 7 and 2 prior to performing retrieval of the materials. Mouse femur samples were immersed in a 4 % paraformaldehyde solution and fixed for 24 h, then specimens were dehydrated, embedded, and sectioned.

BMSC preparation and differentiation

BMSCs were isolated from 6-week-old C57BL/6 mice and characterized as shown previously [29]. BMSCs were induced to osteogenic or adipogenic differentiation according the published methods [29].

Cell Counting Kit-8 (CCK-8)

BMSCs were seeded in 96-well plates at 2×10^3 cells/well and treated with various concentrations of recombinant irisin (0.1, 1, 5, 10, and 20 ng/ml; Enzo Life Sciences, China), respectively. Cell proliferation was assessed on days 1, 3 and 5 using the CCK-8 assay. Optical density (OD) was measured at 450 nm (Bio-Tek, USA).

Preparation of the conditional medium

The BMSCs were differentiated into adipocytes in the presence of irisin (5 ng/ml). After 14 days of induction, cells were cultured in complete DMEM for an additional 3 days. The supernatant was collected and termed conditioned medium (CM), which was mixed with the osteogenic medium to induce osteogenesis at a ratio of 1:1.

Alkaline phosphatase (ALP) and alizarin red s (ARS) staining

On days 7 and 14 post the osteogenic induction, BMSC-differentiated osteoblasts were subjected to ALP and ARS staining and quantified as previously described [29].

Oil Red O (ORO) staining and quantification

Two weeks post the adipogenic induction, BMSC-derived adipocytes were fixed and incubated in ORO staining solution (OriCell, USA). The adipocytes were recorded by a microscope (Zeiss, Germany). Positive areas were quantified using ImageJ software.

Quantitative real-time PCR (qRT-PCR)

Total RNA was extracted from the cells using TRIzol (TaKaRa, Japan) and quantified using a NanoDrop (Thermo Fisher, USA). Reverse transcription was conducted utilizing a reverse transcription kit (ABM, Canada), and qRT-PCR utilizing SYBR Green (BIO-RAD, USA). *GAPDH* was used for normalization, and relative gene expression levels were estimated as the previous method [29]. The sequence of the mouse primers was listed in **Supplementary Table 1**.

RNA sequence

Total RNA from adipocytes derived from BMSCs cultured for 14 days with or without irisin was prepared, and integrity was assessed using a Bioanalyzer (Agilent Technologies, USA). Transcriptome sequencing and analysis were performed by OE Biotech Co. (Shanghai, China). Relevant gene sets were obtained from https://www.ncbi.nlm.nih.gov/, GeneCards-Human Genes, Gene Database, Gene Search, and HALL-MARK_INFLAMMATORY RESPONSE [33].

Western blot

Total protein from the BMSC-derived adipocytes was collected. Proteins were separated and transferred to nitrocellulose membranes (NC) by 10 % SDS-PAGE. Subsequently, NC were incubated in primary antibodies, which included IL-6, TLR4, TLR8, Myd88, NF-κB, phosphor-NF-κB, VCAM1, RUNX2, OCN, and Osterix antibody (Abcam, USA, **Supplementary Table 2**). Subsequently, the NC membranes were second incubated with the appropriate secondary antibodies. Target bands were imaged by a chemiluminescent instrument (Bio-Rad, USA). Data quantification was performed using the Image] software.

Immunofluorescent (IF) staining

The tissue slides from the frozen section and the fixed cells cultured in 24-well plates were incubated with primary antibodies (Abcam, Cambridge, UK; **Supplementary Table 2**), followed by incubation with the secondary antibodies, and counterstained with DAPI in mounting media. Images were recorded under a microscope (Zeiss, Germany).

Statistical analysis

All data in this study were expressed as mean \pm standard deviation and statisticed with GraphPad Prism 8.3.0 software (GraphPad Software Inc. USA). Two groups were analyzed using unpaired Student's t-tests and four groups were analyzed using one-way analysis of variance (ANOVA). A difference of p < 0.05 is considered significant, and *p < 0.05, **p < 0.01, ***p < 0.001, and ****p < 0.0001.

Results

Irisin deficiency exacerbated HFD-induced obesity and fat content

After WT and FNDC5^{-/-} mice were fed with HFD or SD for 10 weeks, we observed an augmentation in body size and body mass of the HFD mice compared with the corresponding SD mice (Fig. 1A, B). ORO staining of the femoral shaft sections at the growth plate further showed that the fat content of the bone marrow increased in mice with HFD compared to those with SD. Moreover, higher bone marrow fat content was observed in the FNDC5^{-/-} mice with HFD than that in the WT mice with HFD (Fig. 1C and Fig. S2H). These results showed that endogenous irisin deficiency exacerbates HFD-induced obesity and enhances marrow fat accumulation in the FNDC5^{-/-} mice.

Irisin deficiency worsened HFD-induced bone mass imageologically

Bone morphometric analysis was conducted on the femurs of the mice. Micro-CT images revealed that HFD significantly decreased the trabecular bone content of the FNDC5^{-/-} and WT mice compared with that of the corresponding SD mice (Fig. 2A, B). In addition, irisin deficiency further reduced the trabecular

bone content in the hyperlipidemic mice. Quantitative analysis of the bone parameters revealed significant decreases in BMD, BV/TV, and Tb. N, Tb. Th and Conn. D in the FNDC5^{-/-} and WT mice with HFD than those with SD. Simultaneously, Tb. Sp and SMI increased significantly. Compared to the WT mice with HFD, the BMD, BV/TV, and Tb. Th of the FNDC5^{-/-} mice with HFD decreased, whereas the Tb. Sp levels increased (Fig. 2C). The micro-CT reconstruction results for the cortical bone displayed that HFD and irisin did not affect the microstructures of the cortical bone (Fig. S2A–D).

Irisin deficiency accelerated HFD-induced bone mass histologically

As expected, the histological analysis was similar to the trend observed in the micro-CT scanning. H&E staining showed that HFD decreased trabeculae mass under the epiphyseal plate, in which a disorderly arrangement was displayed. Impressively, irisin deficiency exacerbated the decrease in bone mass (Fig. 3A). Masson staining showed the reduced collagen fibers under the femoral growth plate in the mice with HFD compared to those with SD. The collagen fibers decreased by nearly half in the FNDC5-/- mice with HFD compared with those in the WT mice with HFD (Fig. 3B). Histological findings demonstrated that HFD reduced bone trabecular mass in mice and the lack of irisin exacerbated this phenomenon.

Irisin deficiency amplified HFD-induced decrease in bone formation

To explore new bone formation dynamically, we performed calcein staining of mouse femurs, which the distance of the two fluorescent lines reflected osteogenesis *in vivo*. The osteogenic capacity of the mice with HFD was diminished compared with that of the corresponding mice with SD, and the osteogenic capacity of the

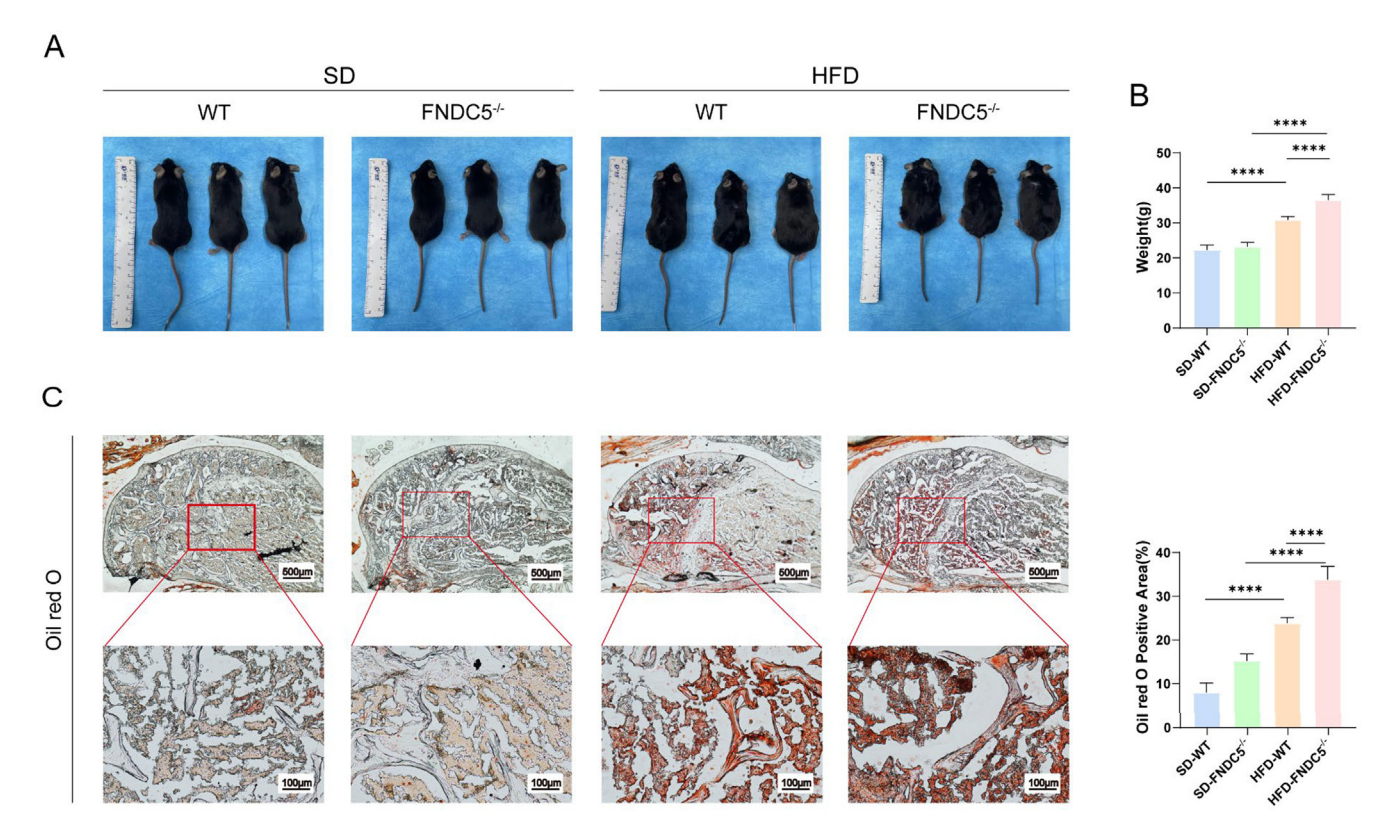


Fig. 1. Irisin deficiency exacerbated HFD-induced obesity and fat content. (A) Gross observation of mice after 10 weeks of dietary intervention. (B) Body mass of the WT and FNDC5 $^{-1}$ - mice. (n = 5) (C) ORO staining and quantification of mouse femur sections. (n = 3).

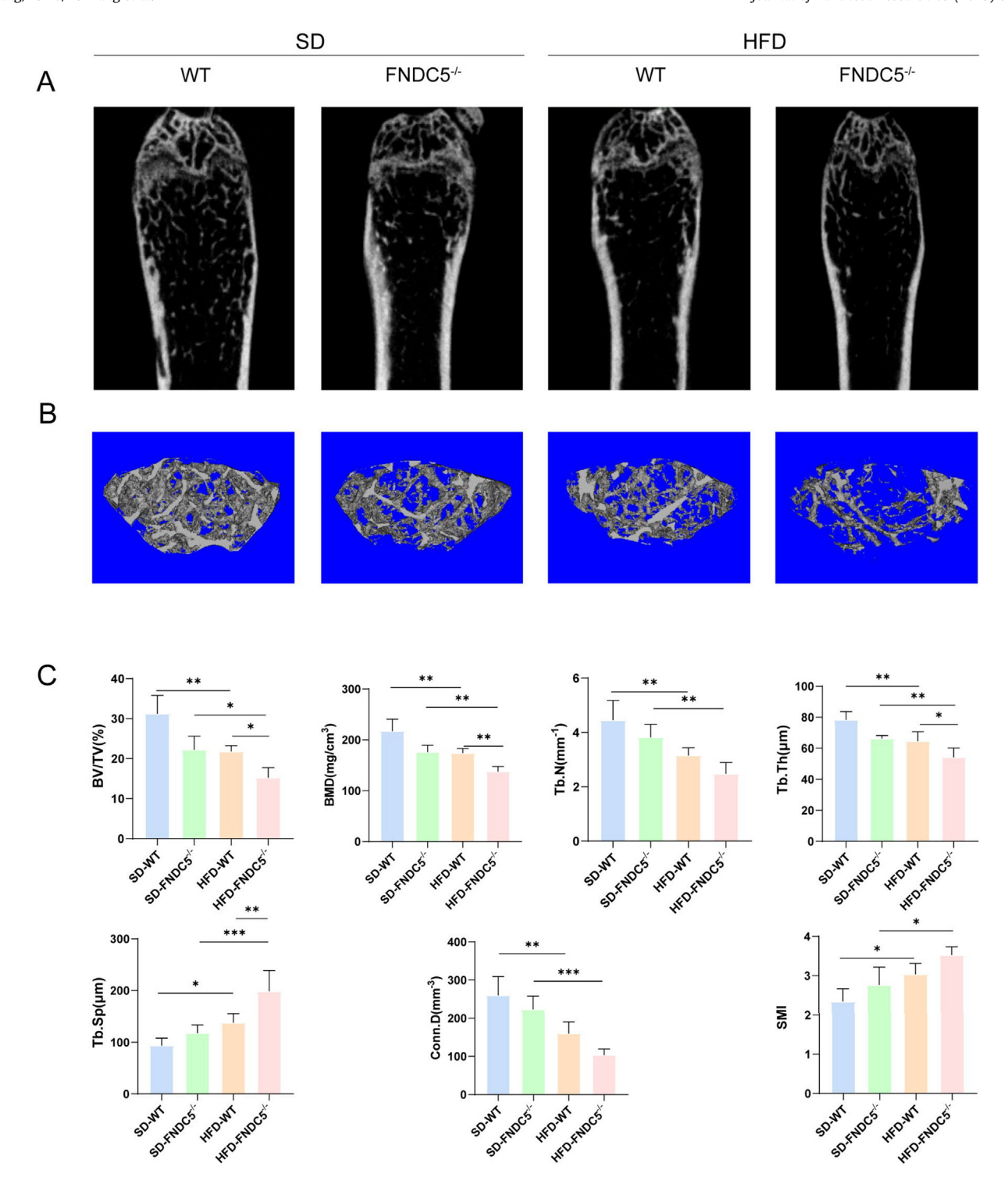


Fig. 2. Irisin deficiency exacerbated HFD-induced bone mass imageologically. The femurs were scanned by Micro-CT. (A) 2D reconstruction of the femurs. (B) 3D reconstruction of the femurs. (C) The trabecular bone parameters included BV/TV, BMD, Tb. N, Tb. Th, Tb. Sp, Conn. D, and SMI. (n = 5).

 $FNDC5^{-/-}$ mice was the most severely impaired among all mice (Fig. 4A, D).

Immunohistochemical (IHC) staining of the distal femurs of mice revealed that, compared with the mice with SD, HFD decreased the number of RUNX2-positive cells along the growth plates of the WT mice by 62 %, and by 44 % in the FNDC5^{-/-} mice (Fig. 4B). In the FNDC5^{-/-} mice with HFD, the number of RUNX2-positive cells was approximately 50 % lower than that in the WT mice with HFD (Fig. 4E). Osterix-positive cell reduction was similar

to that of RUNX2 expression (Fig. 4C, F). HFD decreased the OCN-positive area in the growth plate of the WT mice by nearly one-third, further reduced the OCN-positive area of the FNDC5-/- mice by half (Fig.S2E). In contrast, TRAP staining revealed no significant difference in the number of osteoclasts (Fig. S2F).

We assessed the levels of PINP in mouse serum and observed a significant reduction of PINP levels under the influence of HFD (Fig. 4G). The absence of irisin significantly exacerbated this trend, whereas the change in the serum bone resorption marker CTX was

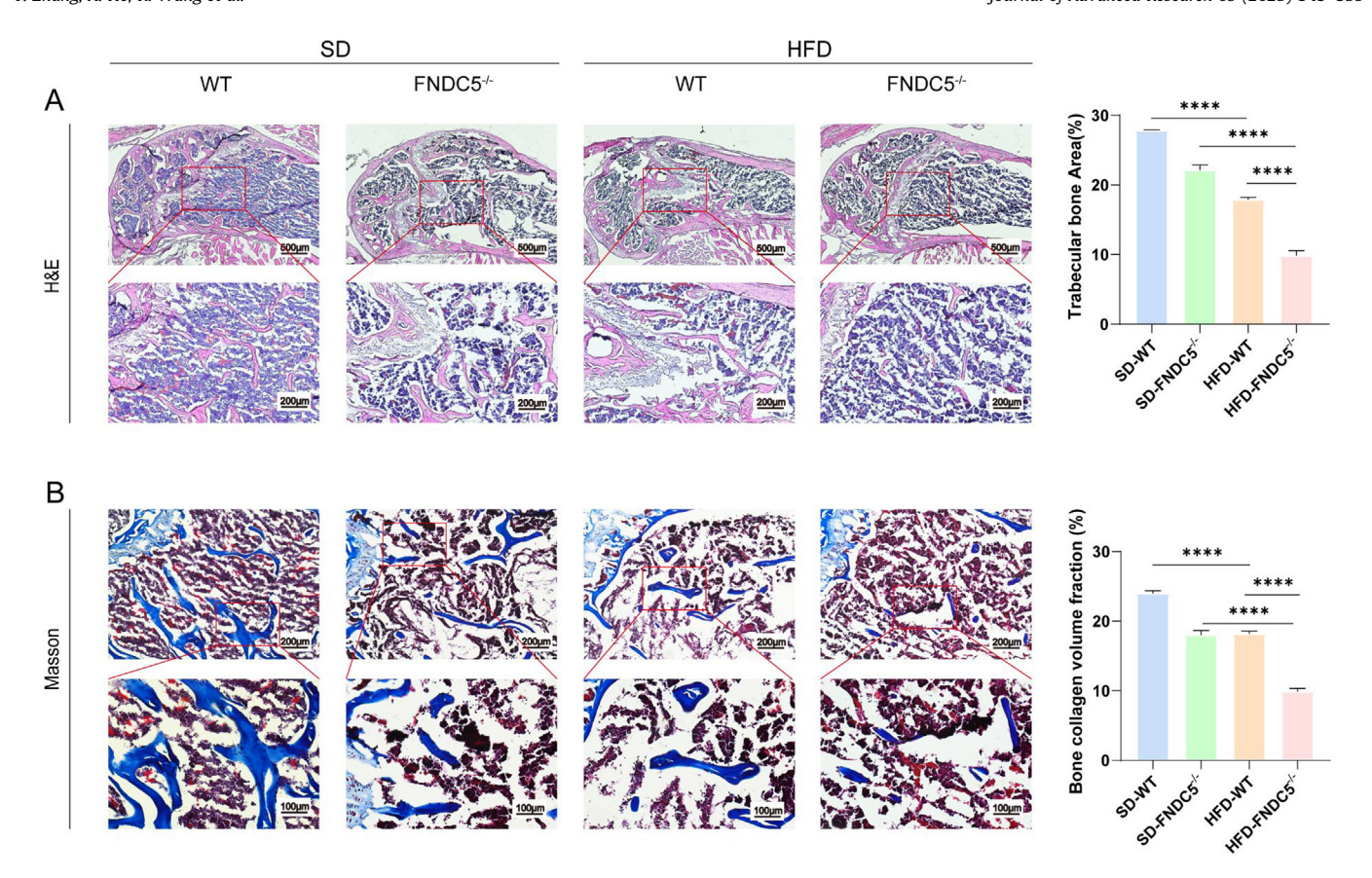


Fig. 3. Irisin deficiency accelerated HFD-induced bone mass histologically. (A) H&E staining of the femur and quantification analysis. (n = 3) (B) Masson staining of the femur and quantification analysis. (n = 3).

not statistically significant (Fig. 4H). These results demonstrated that HFD downregulated the osteogenic ability of mice, and the absence of irisin increased HFD-induced osteogenic ability decrease; however, osteoclast activation was not significantly affected.

Irisin inhibited BMSC-derived adipogenesis

To explore the impacts of bone marrow adipocytes on bone formation, we differentiated BMSCs into adipocytes to mimic BMAT in mice. After identifying the mouse BMSCs using flow cytometry (Fig. S1B), we evaluated the impact of irisin concentration on BMSCs proliferation through a CCK-8 assay. Irisin did not affect the proliferation within 0.1–20 ng/ml (Fig. S1C). Considering the existing literature and our previous research, we chose 5 ng/mL of recombinant irisin to mimic the physiological impact of irisin on adipogenesis [29]. On day 14 after adipogenic induction, ORO staining showed that the number of lipid droplets was significantly increased in BMSC-differentiated adipocytes. Irisin treatment significantly decreased the number of lipid droplets (Fig. 5A, B). Compared with that in the adipogenic group alone, the area of the OROpositive region in the adipogenic group with irisin was reduced by nearly half. The qRT-PCR findings showed that the adipogenesisrelated gene PPARy significantly increased upon the adipogenic induction and decreased by nearly two-thirds in the group with irisin (Fig. 5C).

Irisin alleviated the inhibition of adipocytes on BMSC-derived osteogenesis

To investigate the effect of adipocytes on osteogenesis, BMSCs were subjected to osteogenesis in an osteogenic medium with

50 % CM collected from the adipocytes. After 7 days of osteogenic culture, ALP staining revealed that, compared with the BMSCs with the CM of irisin-incubated adipocytes (CM-(Ad + irisin) group), BMSCs treated with the CM of adipocytes (CM-Ad group) had significantly reduced osteogenic capacity (Fig. 6A, C).

After 14 days of osteogenic culture, the ARS staining results were consistent with those of ALP staining. The number of mineralized nodules in the BMSC-differentiated osteoblasts noticeably decreased in the CM-Ad group. Conversely, the CM-(Ad + irisin) group exhibited partial restoration of the mineralized nodules inhibited by the CM of adipocytes (Fig. 6B, D).

The qRT-PCR results demonstrated that the gene expression of *Alp, Opn, Runx2*, and *Osterix* were significantly lower in the CM-Ad group than those in the standard osteogenic medium (CM-Control, Fig. 6E–H), suggesting that the adipocyte supernatant significantly reduced the osteogenesis of BMSCs. However, these gene expressions in the CM-(Ad + irisin) group were higher than those in the CM-Ad group. Thus, the addition of irisin during adipocyte induction restored the osteogenic ability of BMSCs impaired by the adipocyte supernatant to some extent.

Irisin reduced adipocytes to secrete inflammatory factor

Based on the fact that irisin suppressed adipogenesis, we performed RNA sequencing of adipocytes with and without irisin incubation. We analyzed differentially expressed genes (DEGs) and generated a volcano plot. Since obesity is associated with chronic inflammation, we compiled a list of inflammation-related genes by screening and identified significantly altered inflammation-related genes in the volcano plot (Fig. 7A). Upon irisin addition, genes in adipocytes, such as *Has2*, *Il1r1*, *Il-6*, *Myc*, *Tnfaip6*, *Nampt*, *Slc7a2*, and *Vcam1* were downregulated, while *Cal*-

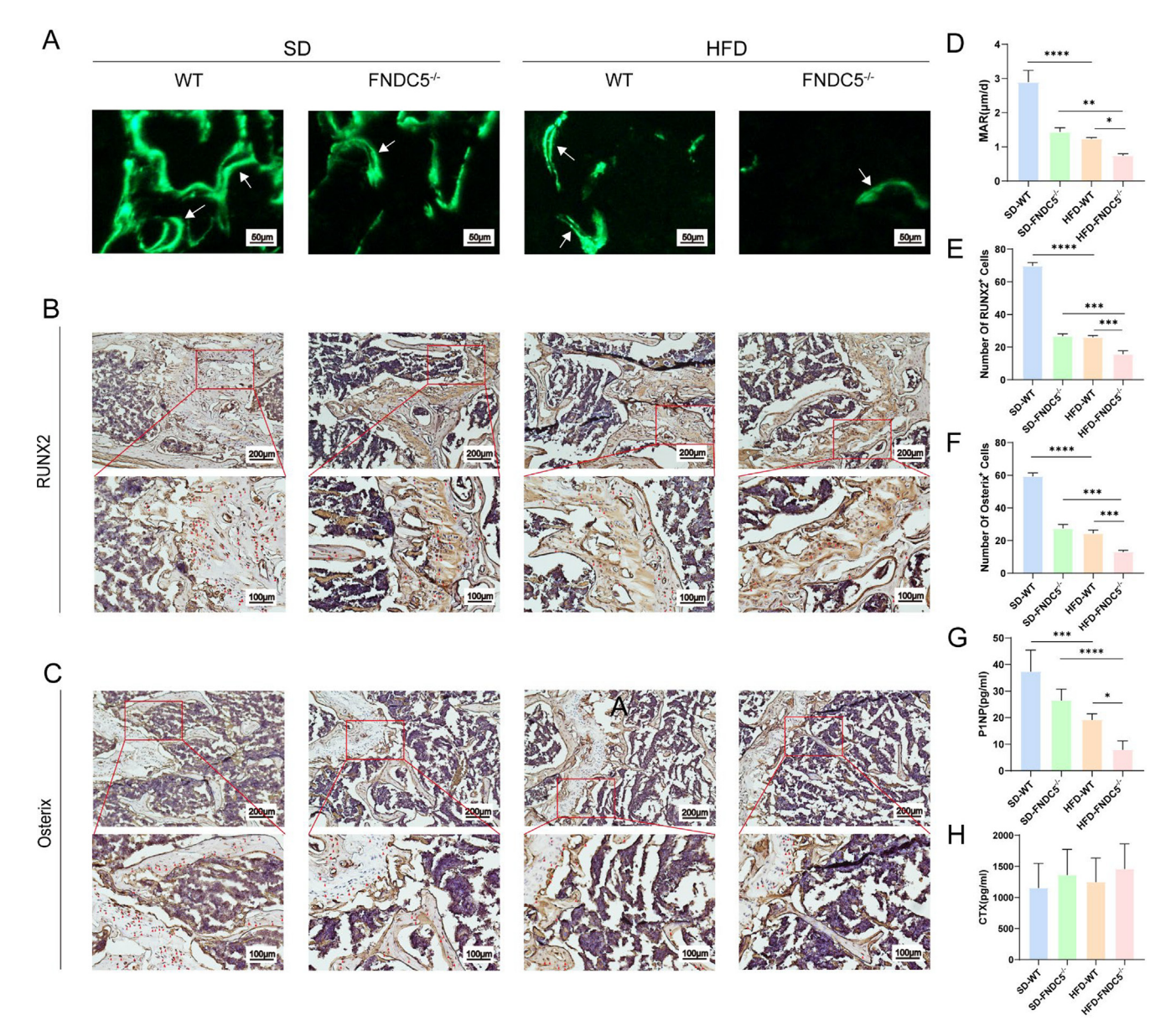


Fig. 4. Irisin deficiency exacerbated the decrease in bone formation induced by HFD. (A) Representative images of calcein fluorescent staining. (B) RUNX2 expression in femur detected by IHC. (C) Osterix expression in femur detected by IHC. (D) The mineralized deposition rate (MAR) of bone trabeculae was quantified. (n = 3) (E) Quantitative analysis of RUNX2* cells. (n = 3) (F) Quantitative analysis of Osterix * cells. (n = 3) (G) PINP in sera by ELISA. (n = 5) (H) CTX in sera by ELISA. (n = 5).

crl and *Il18r1* were upregulated (Fig. 7A). Subsequently, we generated an expression profile of the inflammation-related genes based on the screening results (Fig. S1D). Utilizing the Gene Ontology (GO) database, a Gene Set Enrichment Analysis (GSEA) was performed on the inflammation response data. The analysis revealed that the hormone irisin has a downregulating effect on the inflammation response (Fig. S1E). In the gene heatmap, the expression of genes associated with inflammation was reduced after irisin treatment (Fig. 7B). Therefore, we hypothesized that irisin would downregulate adipocyte inflammation.

To investigate the pathways through which irisin exerts its antiinflammatory effects, we focused on the top 30 related pathways downregulated in the KEGG analysis (Fig. 7C). In the bubble plot, we observed significant changes in the NF-κB and TLR pathways. The GSEA analysis based on kyoto encyclopedia of genes and genomes (KEGG) data revealed that the addition of irisin inhibited the NF-κB and TLR pathways (Fig. S1F, G). Subsequently, we analyzed the gene expression profiles related to the NF-κB and TLR signaling pathways. We found that the addition of irisin significantly down-regulated the genes related to these two pathways (Fig. 8A,B). We also performed a GO enrichment analysis of the genes downregulated after irisin treatment (Fig. 8C). The top 15 BP (Biological Process), CC (Cell Component), and MF (Molecular Function) with the most significant differences were selected and displayed in the results. The production of IL-6 in the cytoplasmic vesicles, extracellular space, and extracellular regions was significantly downregulated.

To investigate the interactions between the most significantly different genes and pathways with the most significant changes, we conducted gene enrichment and created chord diagrams based on KEGG enrichment (Fig. 8D). Genes Vcam1, Tlr8, and Il-6 were significantly downregulated and were positively related to the NF- κ B and TLR pathways.

In the gene enrichment and chord diagram of WikiPathways, *Il-6* gene expression underwent significant changes and was closely associated with the fat generation pathway (Fig. S1H).

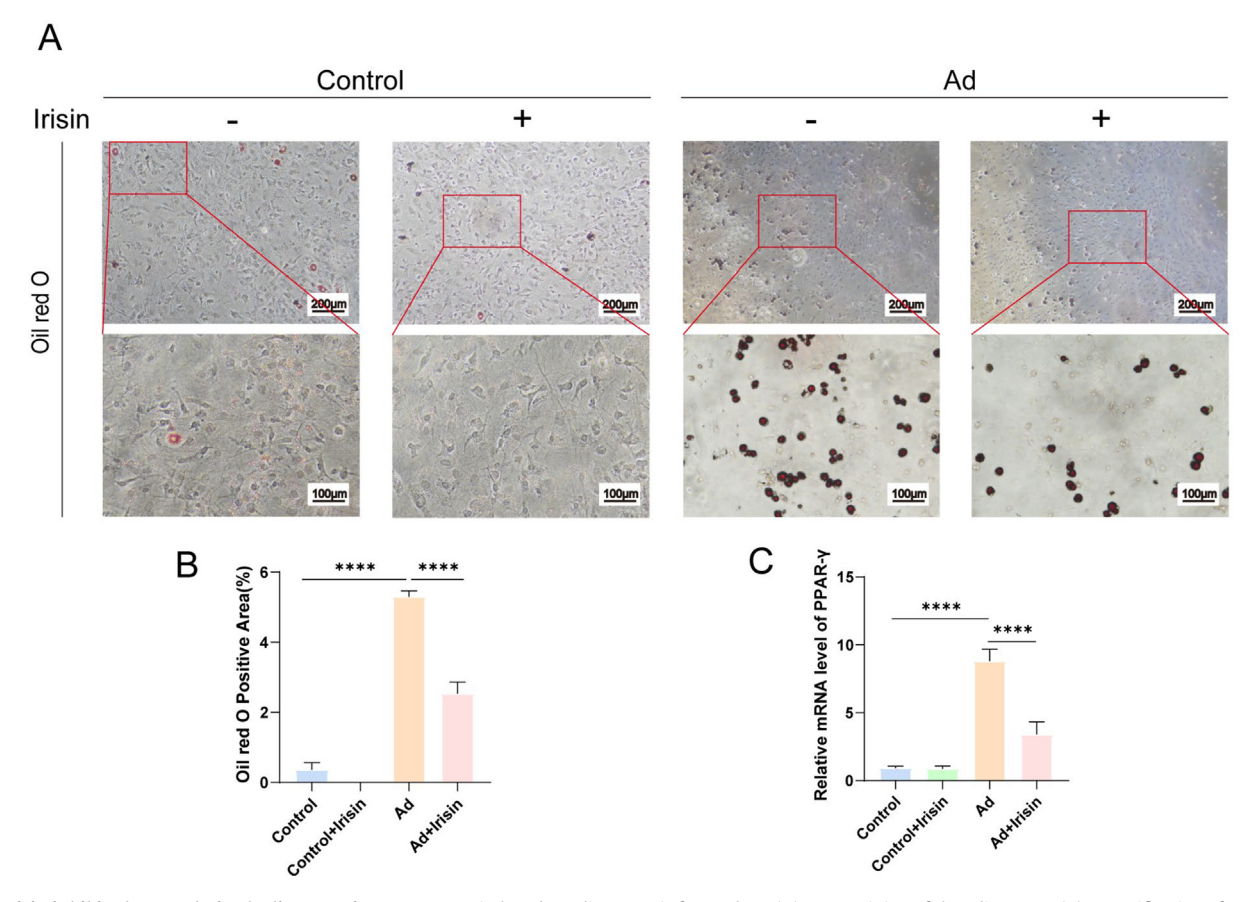


Fig. 5. Irisin inhibited BMSC-derived adipogenesis. BMSCs were induced to adipogenesis for 14 days. (A) ORO staining of the adipocytes. (B) Quantification of ORO staining of the adipocytes. (n = 3) (C) *PPARγ* gene expression in adipocytes by qRT-PCR. (n = 3).

Based on the RNA sequence data of adipocytes, we hypothesized that irisin could affect the ability of BMSCs to differentiate toward osteoblasts by inhibiting the secretion of inflammatory factors in adipocytes. We also speculated that the NF- κ B and TLR pathways might closely mediate the production of IL-6.

Irisin suppressed adipocytes to secrete IL-6 via the TLR4/MyD88/NF- κB pathway

We scrutinized the RNA sequencing results and verified substantial alterations in genes and pathways with qRT-PCR and discovered that the changes in the inflammatory factors $\mathit{Il-6}$ and $\mathit{Vcam1}$ were the most significant during adipogenesis. The expression of $\mathit{Il-6}$ and $\mathit{Vcam1}$ in BMSC-derived adipocytes was higher than that in BMSCs. With the introduction of irisin, the levels of $\mathit{Il-6}$ and $\mathit{Vcam1}$ significantly reduced (Fig. 9A). During the pathway validation process, $\mathit{Tlr4}$, $\mathit{MyD88}$, and $\mathit{NF-\kappa B}$ were significantly upregulated upon adipogenic induction, and irisin decreased the expression of these genes (Fig. 9A). There was no difference in the gene changes of $\mathit{Tlr8}$ (Fig. S2G).

The outcomes from western blot analysis were in line with the qRT-PCR findings, as evidenced by TLR4 and MyD88 being upregulated due to adipogenesis and downregulated following irisin administration (Fig. 9B). The percentage of phosphorylated NF- κ B to total NF- κ B was increased upon adipogenesis and decreased upon irisin addition (Fig. 9B). The trend in downstream IL-6 expression was consistent with the results at the gene level (Fig. 9B). Nevertheless, there was no notable difference in the VCAM1 expression between adipocytes treated with or without irisin (Fig. 9B).

We detected IL-6 secretion into the cell culture supernatant using ELISA. BMSC-differentiated adipocytes secreted more IL-6 than BMSCs. However, the increase in IL-6 levels was significantly reduced following the addition of irisin (Fig. 9C). Therefore, we proposed that phosphorylated NF-κB activated the TLR4/MyD88 signaling pathway in adipocytes to enter the nucleus and activate the *Il*-6 gene to produce IL-6; therefore, by inhibiting NF-κB phosphorylation, irisin reduced IL-6 production.

During adipo-differentiation, irisin significantly reduced IL-6 production in adipocytes, as displayed by co-staining of IL-6 and the cytoskeleton (Fig. 10A). Co-staining results for TLR4 and IL-6 further suggested that irisin reduced the secretion of IL-6 by reducing the expression of TLR4 in adipocytes (Fig. 10B).

To validate this hypothesis, we isolated BMSCs from the FNDC5^{-/-} mice and induced adipogenesis to generate irisin-deficient adipocytes; meanwhile, part of the FNDC5^{-/-} BMSCs were incubated with TLR4 receptor selective inhibitor resatorvid (TAK-242, 1 μ M) during adipogenesis. After confirming the deficiency of FNDC5 expression in BMSC-differentiated adipocytes from the FNDC5^{-/-} mice (Fig. S1I), we performed ORO staining of adipocytes to observe the adipogenic potential of BMSCs. As expected, the adipogenic ability of the BMSCs from the FNDC5^{-/-} mice was higher than those from the WT mice. TAK-242 did not affect adipogenesis of BMSCs either from the FNDC5^{-/-} or WT mice (Fig. 11A).

Next, we collected the supernatant of the BMSC-differentiated adipocytes as a conditioned medium to investigate the crosstalking effect of adipocytes on BMSC osteogenesis. Irisin deficiency intensified the inhibition of osteogenesis by the adipocyte supernatant, whereas the addition of TAK-242 rescued the inhibition of osteogenesis by the adipocyte supernatant (Fig. 11B, C). The

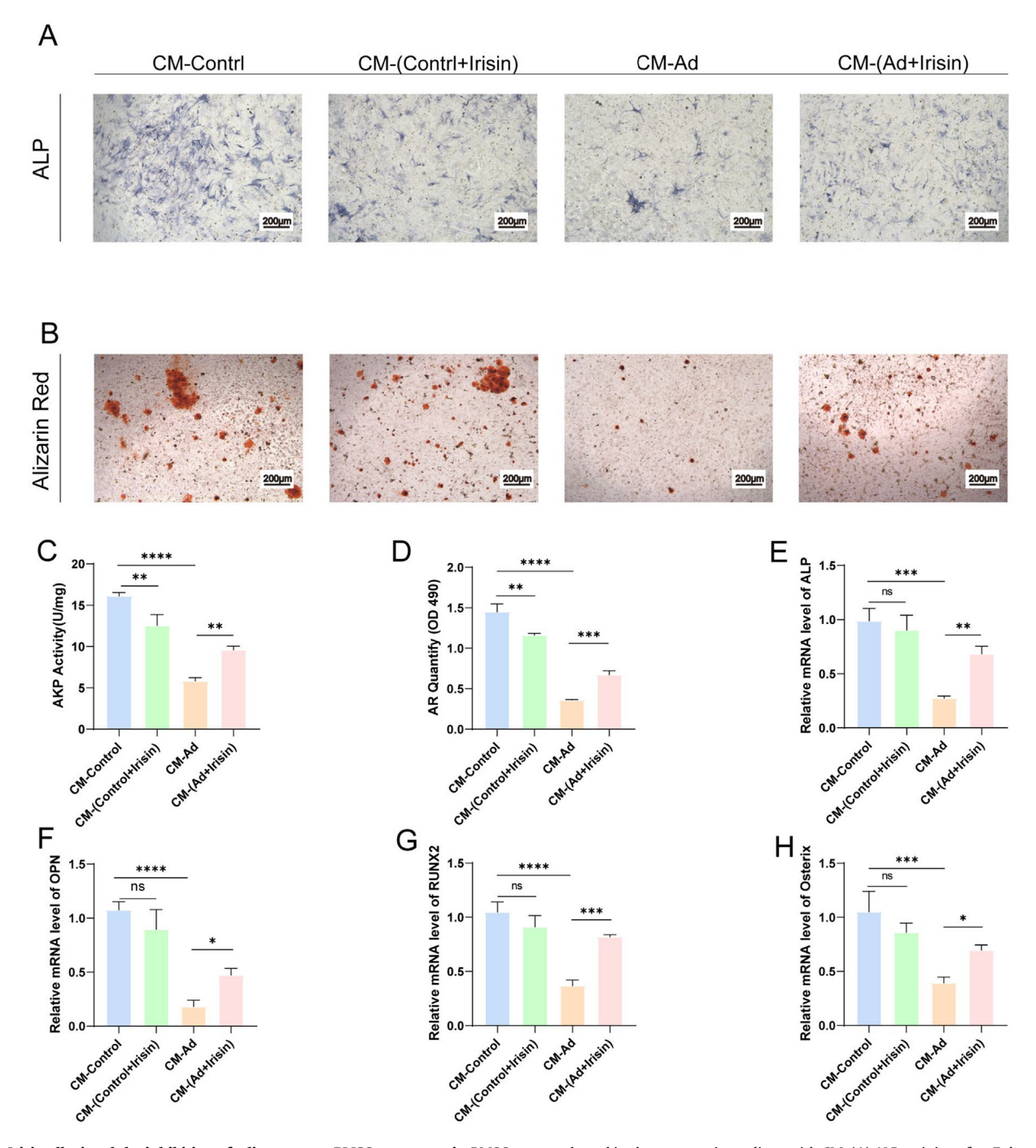


Fig. 6. Irisin alleviated the inhibition of adipocytes on BMSC osteogenesis. BMSCs were cultured in the osteogenic medium with CM. (A) ALP staining after 7 days. (B) ARS staining after 14 days. (C) Quantification of ALP activity. (n = 3) (D) Quantitative of mineralized nodules. (n = 3) (E-H) Gene expression of *Alp, Opn, Runx2*, and *Ostrix* detected by qRT-PCR after 7 days. (n = 3).

qRT-PCR results displayed a significantly higher expression of the $\it Il-6$ gene in adipocytes of the FNDC5- $\it Il-6$ mice than that in the WT mice.

Concurrently, treatment with TAK-242 statistically suppressed the expression level of $\it ll-6$ (Fig. 11D). The gene expression trend of $\it Tlr-4$, $\it MyD88$ as well as $\it NF-\kappa B$ was also consistent with $\it ll-6$ gene expression (Fig. 11D). In terms of protein expression, TLR4/MyD88 and phosphorylated NF- $\it \kappa B$ were upregulated in the absence of irisin and downregulated upon addition of TAK-242 (Fig. 11E). In sum, these results showed that irisin downregulated the TLR4/

MyD88 signaling pathway, consequently reduced NF- κ B phosphorylation to decrease the production of IL-6.

Irisin deficiency increased TLR4 and IL-6 expression in the bone marrow cavity of HFD mice

We performed IF staining of bone marrow sections, and found an increased expression of IL-6 and TLR4 in the bone marrow of the WT mice with HFD compared to that with SD (Fig. 12A, B). Notably, irisin deficiency exacerbated this effect. Thus,

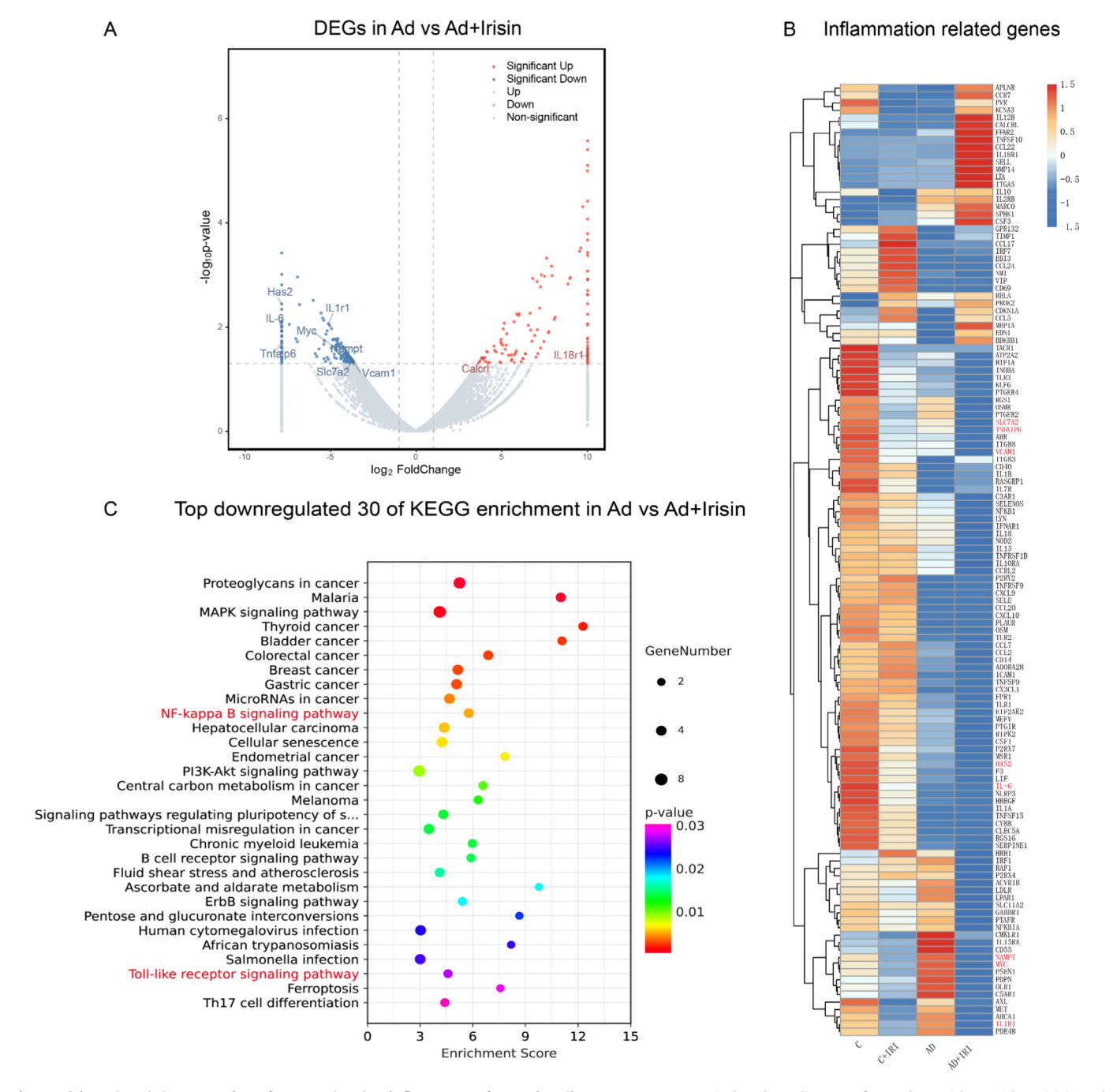


Fig. 7. Irisin reduced the expression of genes related to inflammatory factors in adipocytes. BMSCs were induced to adipocytes for 14 days with or without irisin and RNA-sequence were performed. (A) Volcano plot showing differentially regulated genes. (B) Heatmap showing inflammation-related gene expression. (C) KEGG enrichment analysis.

irisin reduced the production of IL-6 through the TLR4/ MyD88 signaling.

Discussion

Bone metabolism is regulated by bone homeostasis and the bone marrow microenvironment [34]. Accumulating evidence affirms that obesity is deeply involved in osteoporosis [35]; however, its relevant mechanism should be strongly emphasized. In this study, we fed the FNDC5^{-/-} mice with HFD to explore the impact of irisin on bone metabolism. First, we observed that irisin deficiency increased the body weight and fat content in the bone

marrow of the FNDC5^{-/-} and WT mice with HFD, compared to the corresponding mice with SD. In addition, irisin deficiency aggravated bone loss and impaired the osteogenic ability of the mice with HFD. *In vitro*, irisin inhibited the adipogenic differentiation of mouse BMSCs. Meanwhile, the adipocyte supernatant inhibited the osteogenic differentiation from BMSCs.

As Fig. 6 indicated, irisin suppressed adipogenesis and alleviated adipocyte-induced inhibition of BMSC-derived osteogenesis. We studied the osteogenesis of MSCs with different CM. Compared to the CM control group, we found a slight decrease in osteogenic differentiation in the CM- (Control + irisin) group, while qRT-PCR of osteogenesis-related genes (*Alp, Opn, Runx2, Ostrix*) showed no significant difference between these two groups. Irisin, which

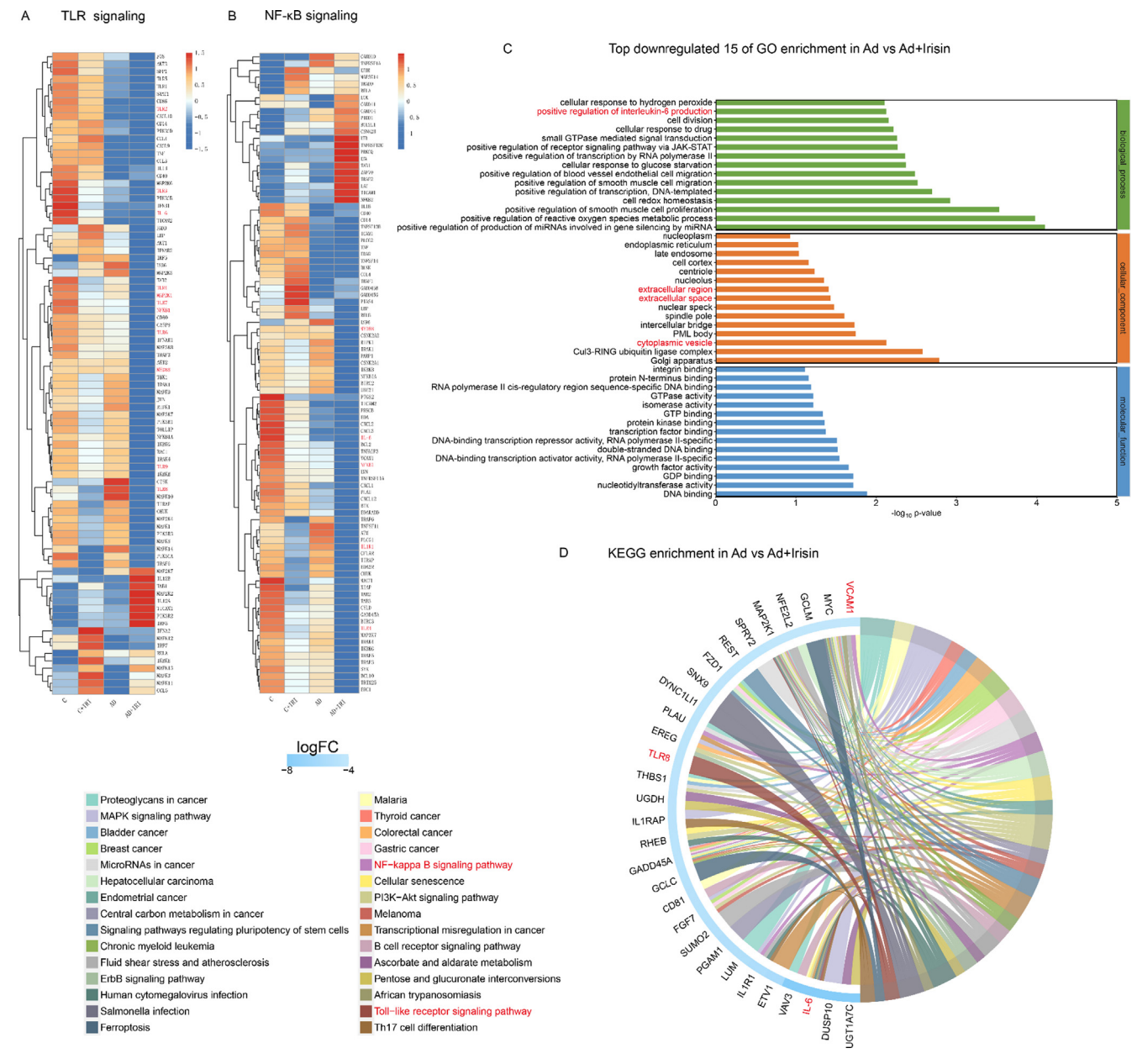


Fig. 8. Irisin downregulated the TLR4/NF-κB pathway in adipocytes. (A) Heatmap showing TLR-related gene expression. (B) Heatmap showing NF-κB-related gene expression. (C) GO enrichment analysis of differential genes. (D) Chord diagram showing KEGG enrichment analysis.

promotes cellular energy metabolism and increases the uptake of nutrients by BMSCs, is associated with exercise [36–39]. Compared to the control group, the addition of irisin may have led to an increase in the uptake of nutrients in the culture medium by BMSCs. This may be the reason for the slightly lower osteogenic effect observed in CM- (Control + irisin) compared to CM-(Control), even though CM was prepared 3 days after replacing the old cell medium with fresh cell medium. Furthermore, in vitro study verified that irisin reduced the secretion of IL-6 in adipocytes by downregulating TLR4/my88/NF-κB pathway, consequently, alleviated the osteogenic inhibition caused by the adipocyte supernatant. Furthermore, there was an increased expression of IL-6 and TLR4 in the bone marrow of the FNDC5^{-/-} mice with HFD compared to the WT mice with HFD. Our experiment identified the impact of irisin on the relationship between bone and fat metabolism and provided new ideas for improving obesity-induced bone loss.

IL-6, an inhibitor of osteogenesis, regulates the activities of MEK2 and Akt2 through SHP2, thereby inhibiting osteogenic differentiation and decreasing bone mineralization [40]. IL-6 can also inhibit osteoblast differentiation by reducing MAPK signaling through JAK/STAT3 [41]. Obesity positively regulates the IL-6 receptor and IL-6 expression [42]. Studies have also indicated a direct correlation between increases in IL-6 and IL-6 receptors with body mass index and body fat percentage [43]. In addition, IL-6 gene knockout helps mice resist bone loss caused by HFD [44]. IL-6 may accelerate BMSC aging via the IL-6/STAT3 pathway [45,46]. Secretion of IL-6 promotes cellular senescence [47]. Our study showed that IL-6 secretion in the bone marrow cavity of the FNDC5^{-/-} mice was higher than that of the WT mice, leading to osteoporosis, consistent with previous results. Although IL-6 produced by adipocytes in the bone marrow microenvironment inhibited MSC-derived osteogenesis, irisin mitigated this inhibition by reducing IL-6 production and promoting bone mass.

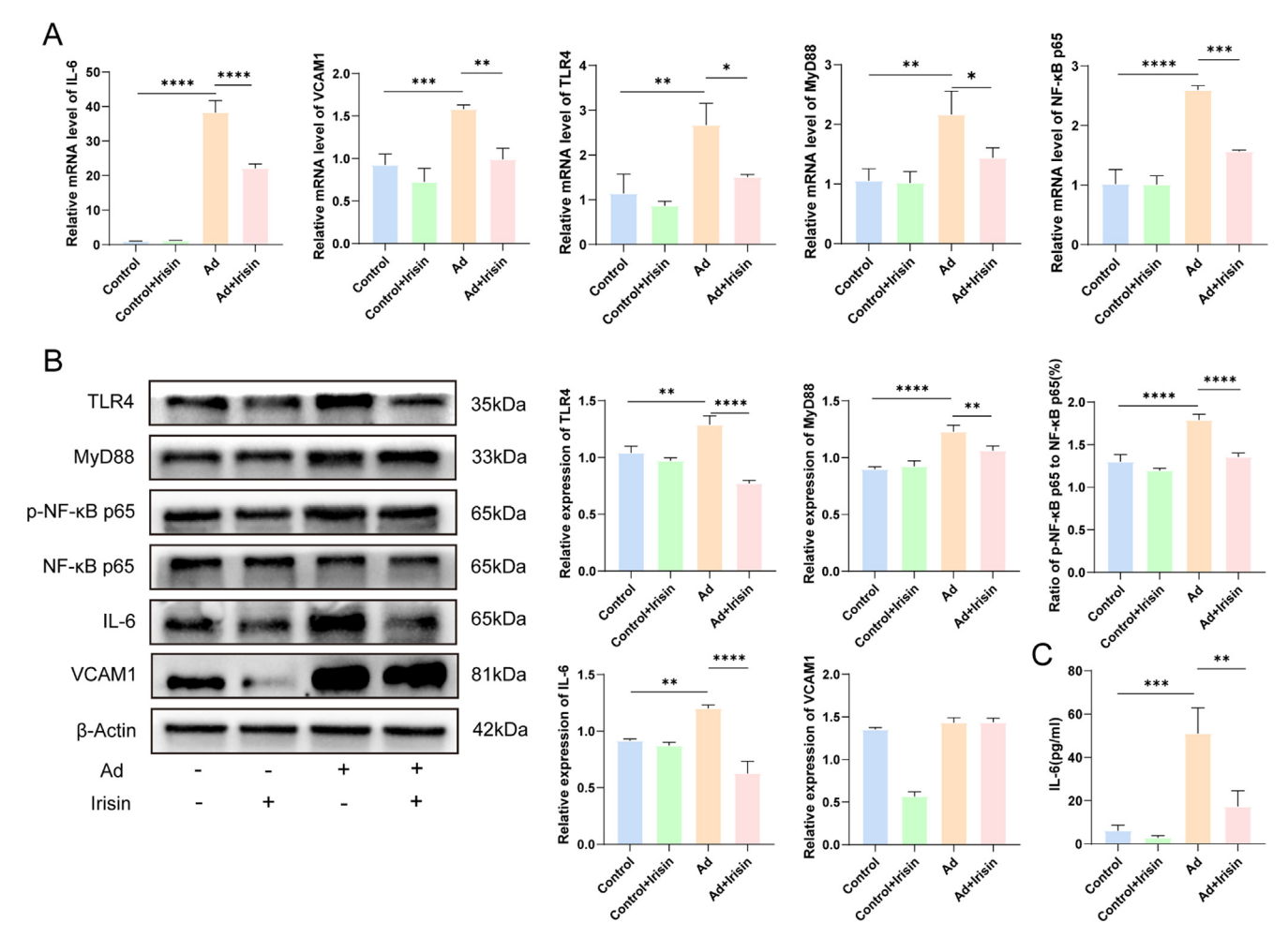


Fig. 9. Irisin suppressed BMSC-differentiated adipocytes to secret IL-6 though the TLR4/NF-κB pathway. (A) Gene expressions of *Il*-6, *Vcam1*, *Tlr4*, *MyD88*, and *NF-κB* detected by qRT-PCR. (n = 3) (B) Protein expressions of IL-6, VCAM1, TLR4, MyD88, and NF-κB detected by WB. (n = 3) (C) IL-6 in the cell supernatant determined by ELISA. (n = 5).

Irisin, an exercise-induced factor originating from its precursor FNDC5, is secreted by muscles and exerts various biological functions through several signaling pathways [48,49]. Irisin can inhibit fat production through the WNT/ β -catenin signal [50] and enhance osteoblast differentiation by activating the P38 and ERK [51]. However, irisin can impede the activation of osteoclasts by activating the P38 and JNK [52]. A lack of irisin increases osteoclastogenesis [53]. Our previous research also confirmed that irisin can promote osteogenic differentiation by activating the BMP/SMAD signaling pathway in BMSCs through αV integrin receptors [29] and condition the balance between osteogenesis and osteoclastogenesis by inhibiting oxidative stress and RANKL generation [30].

By RNA sequencing, we showed that irisin affected the secretion of IL-6 in adipocytes, which was related to the TLR/NF-κB pathway. The TLR signaling pathway is essential for innate immune responses and critical for inflammation, immune cell regulation, survival, and proliferation. TLR activation in bone marrow-derived fat cells results in the production of inflammatory factors [54]. Chronic inflammation in adipose tissue is associated with the TLR and NF-κB regulatory pathways. Compared with the TLR family TLR 1, 2, 7, and 8, TLR4 has a higher gene expression level in adipose tissue. Irisin protects the brain from I/R-induced inflammatory injury by inhibiting the TLR4/MyD88 pathway [55]. Research has demonstrated that irisin effectively reduces IL-6 production and diminishes the activation of the TLR4/NF-κB signaling pathway with inflammatory stress [26,56,57]. Conversely, another

study highlights that irisin can activate NF-κB in adipocytes, subsequently promoting the release of CXCL1 [58]. These findings elucidate the cell-type specific effects of irisin on NF-κB activity, indicating its versatile role in different cellular contexts. Overall, our study showed that bone loss induced by obesity may be closely related to the TLR4/NF-κB signaling pathway and the inflammatory cytokine IL-6, and the application of recombinant irisin can alleviate the bone loss induced by obesity. Irisin could reduce the production of IL-6 in adipocytes in the bone marrow through the TLR4/MyD88/NF-κB pathway, consequently preventing bone loss caused by obesity. Therefore, irisin, as a therapeutic agent for the treatment of obesity-induced bone loss, provides new pathway insights for the clinical treatment of obesity-induced bone loss.

Of course, our study had some limitations. Bone metabolism is closely related to the Hedgehog signaling pathway, Notch signaling pathway, Wnt/ β -catenin signaling pathway, TGF/BMP signaling pathway and FGF signaling pathway. Alterations in the gut microbiota have a significant regulatory role in the musculoskeletal system [59–61], especially bone loss caused by obesity [62]. In this study, we found that the TLR4/NF- κ B signaling pathway plays an important role in obesity-induced bone loss, which is closely related to the production of the inflammatory cytokine IL-6. Moreover, the application of recombinant irisin can improve the bone loss caused by obesity, and the mechanism of how irisin affects the TLR4/NF- κ B signaling pathway and improves the bone loss needs to be further investigated in subsequent studies. Irisin can

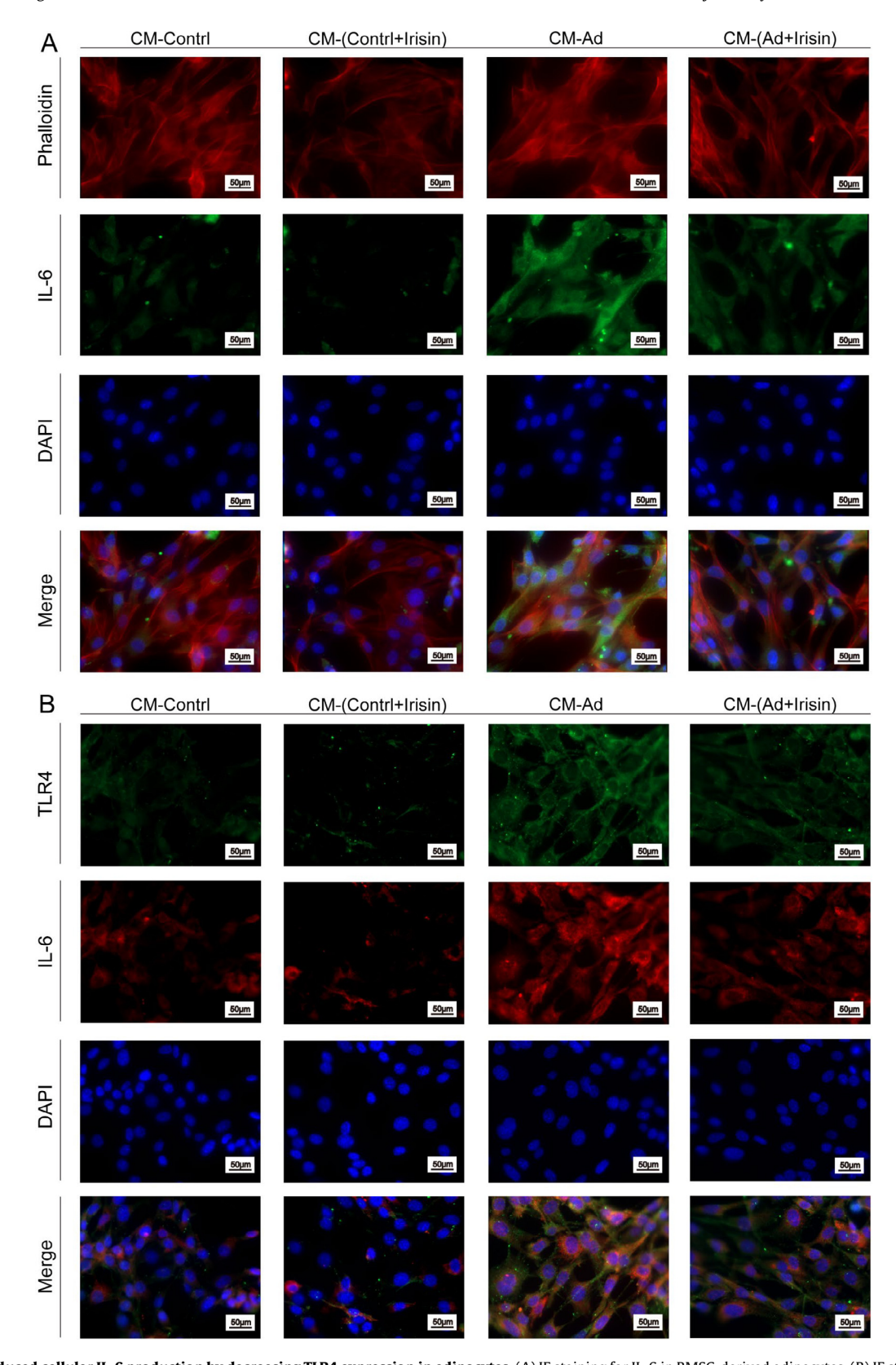


Fig. 10. Irisin reduced cellular IL-6 production by decreasing TLR4 expression in adipocytes. (A) IF staining for IL-6 in BMSC-derived adipocytes. (B) IF staining for IL-6 and TLR4 in BMSC-derived adipocytes.

influence both bone and fat metabolism via αV integrin receptors [29,63]. However, it remains unconfirmed whether irisin impacts the TLR4/NF- κB signaling pathway in adipocytes through these receptors or by binding to other receptor proteins. Moreover, we

will delve into the specific receptor that irisin binds to and its binding mode, to further elucidate how irisin mitigates adipose-induced osteogenesis inhibition via its effect on the TLR4/NF- κ B signaling pathway in adipocytes. The utilization of FNDC5 gene

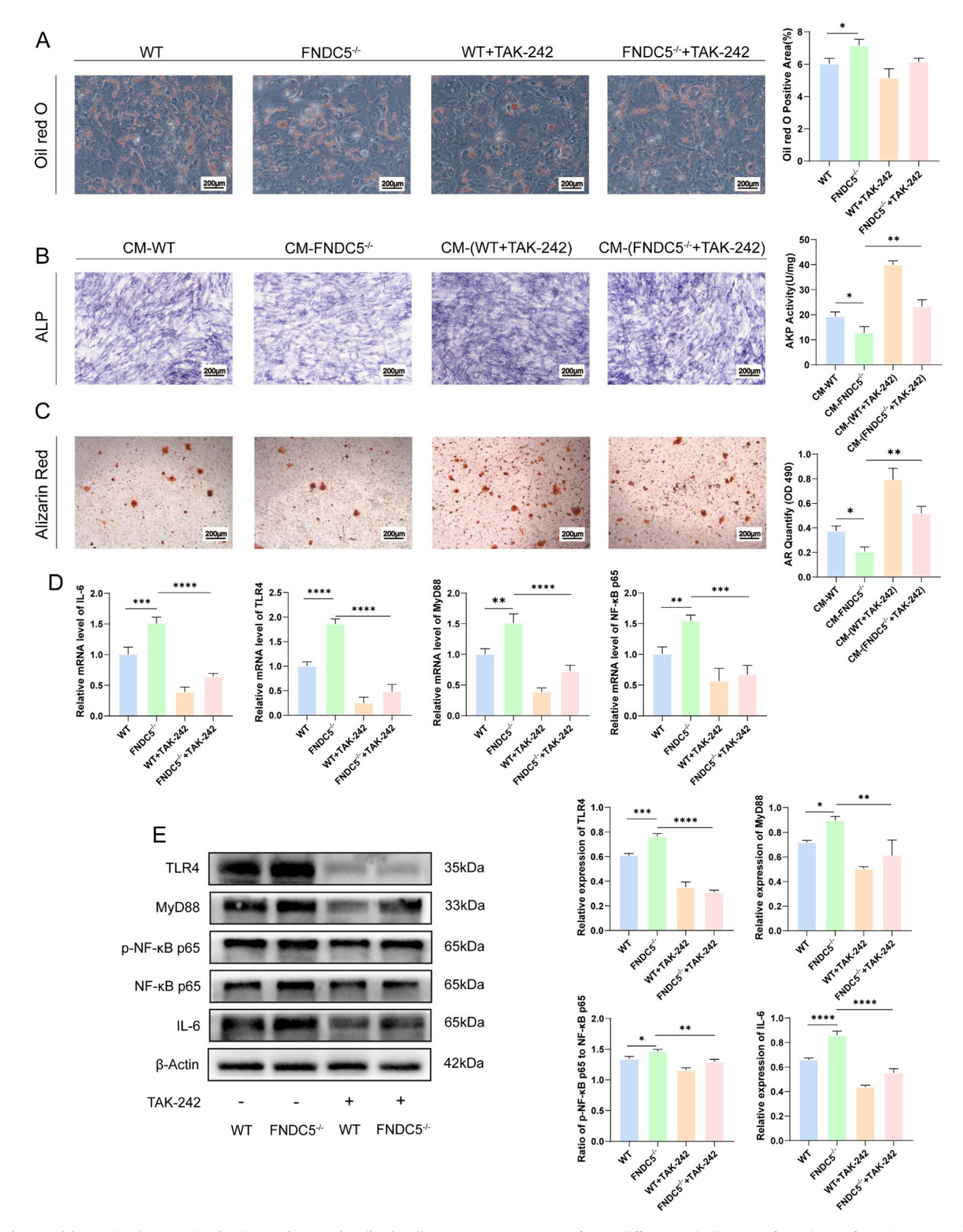


Fig. 11. Irisin regulated IL-6 production by TLR4/MyD88 signaling in adipocytes. (A) ORO staining of BMSC-differentiated adipocytes after induction for 14 days. (n = 3) (B) ALP staining and ALP activity of BMSC-differentiated osteoblasts 7 days after cultured with the osteogenic conditional medium. (n = 3) (C) ARS staining and quantification of mineralized nodules of BMSC-differentiated osteoblasts 14 days after cultured with the osteogenic conditional medium. (n = 3) (D) The gene expression of *Il-6, Tlr-4, MyD88* and *NF-κB* detected by qRT-PCR. (n = 3) (F) The protein expression IL-6, TLR-4, MyD88 and NF-κB detected by WB. (n = 3).

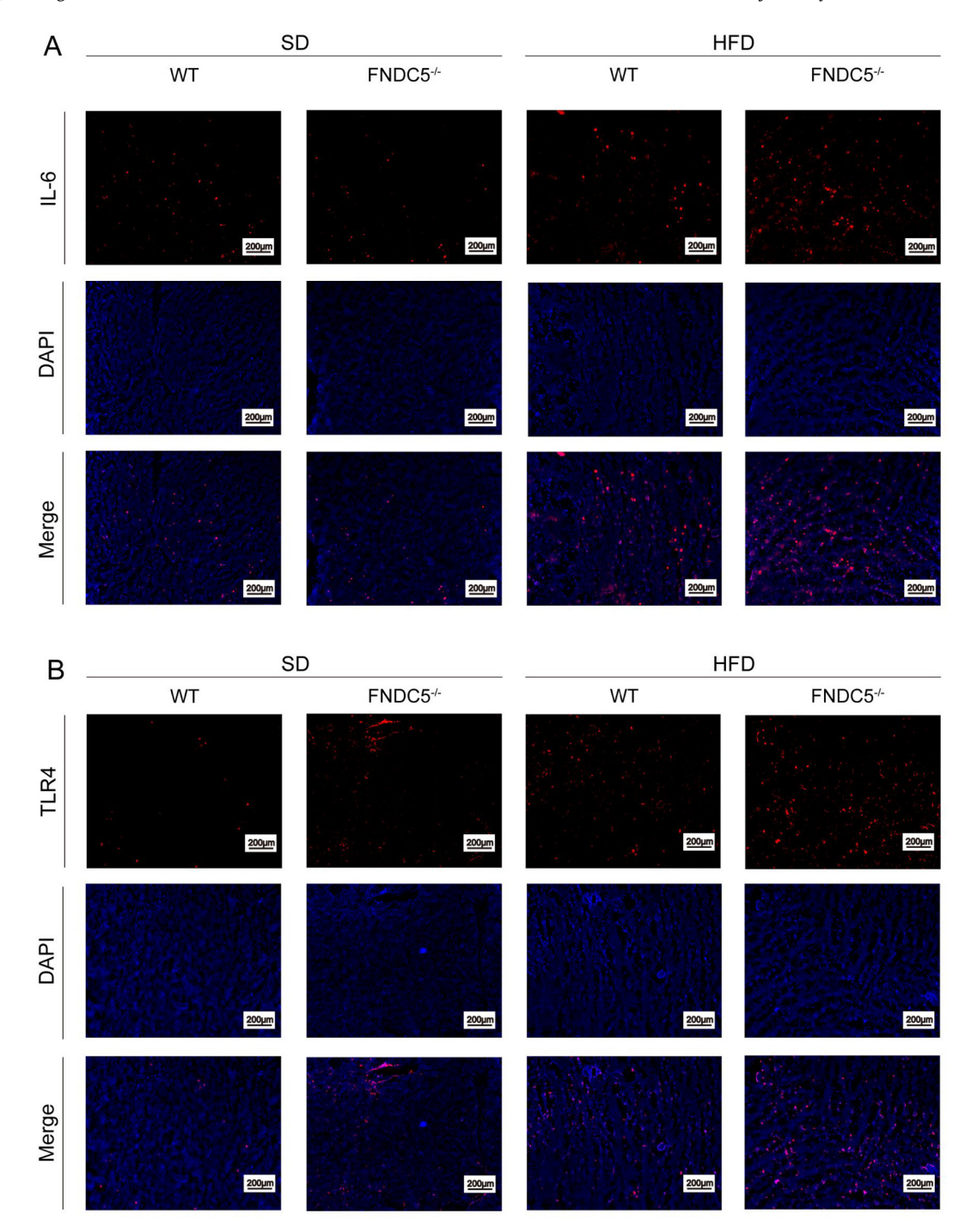


Fig. 12. Irisin deficiency increased TLR4 and IL-6 expression in the bone marrow cavity of the mice. (A) IF staining of IL-6 in the femur. (B) IF staining of TLR4 in the femur.

knockout mice may influence the physiological activities of multiple tissues, including nerves, skeletal muscles, and adipose tissue [64]. Lack of irisin directly affects bone balance. In subsequent investigations, we intend to generate FNDC5 conditional knockout mice to conduct a more precise and detailed exploration, particularly focusing on the mechanisms underlying the interplay between bone and fat metabolism.

the osteogenic capacity that was inhibited by IL-6 . Overall, this series of studies not only enhances our understanding of communication between adipocytes and osteocytes, but also provides new directions for irisin-based therapeutic strategies to modulate bone health.

the activation of the TLR4/MyD88/NF-κB pathway in adipocytes,

thereby decreasing the secretion of IL-6 in adipocytes and restoring

Conclusion

In conclusion, this study demonstrates that irisin deficiency leads to increased obesity-related bone loss. The application of recombinant irisin affected bone and fat metabolism and inhibited

Compliance with Ethics Requirements

The Animal Care and Use Committee of Soochow University approved all experimental animal procedures related to this study (KS2023032).

Declaration of competing interest

The authors declare that they have no known competing financial interests or personal relationships that could have appeared to influence the work reported in this paper.

Acknowledgments

This work was supported by grants from the Wuxi Top Medical Expert Team of the Taihu Talent Program, National Natural Science Foundation of China (82372457,82172485), Technology Innovation on Medicine and Health of Suzhou Science and Technology Bureau (SKY2022041), Orthopaedic Medical Innovation Center of Jiangsu (CXZX202209), and Key Laboratory of Orthopaedics of Suzhou (SZS2022017).

Appendix A. Supplementary data

Supplementary data to this article can be found online at https://doi.org/10.1016/j.jare.2024.04.013.

References

- [1] Finkelstein EA, Khavjou OA, Thompson H, Trogdon JG, Pan L, Sherry B, et al. Obesity and severe obesity forecasts through 2030. Am J Prev Med 2012;42 (6):563–70.
- [2] Kelly T, Yang W, Chen CS, Reynolds K, He J. Global burden of obesity in 2005 and projections to 2030. Int J Obes (Lond) 2008;32(9):1431–7.
- [3] Wang YC, McPherson K, Marsh T, Gortmaker SL, Brown M. Health and economic burden of the projected obesity trends in the USA and the UK. Lancet 2011;378(9793):815–25.
- [4] Piche ME, Tchernof A, Despres JP. Obesity phenotypes, diabetes, and cardiovascular diseases. Circ Res 2020;126(11):1477–500.
- [5] Hannan MT, Felson DT, Anderson JJ. Bone mineral density in elderly men and women: results from the Framingham osteoporosis study. J Bone Miner Res Off J Am Soc Bone Miner Res 1992;7(5):547–53.
- [6] Chen R, Armamento-Villareal R. Obesity and skeletal fragility. J Clin Endocrinol Metab 2023.
- [7] Hu FB. Overweight and obesity in women: health risks and consequences. J Womens Health (2002) 2003;12(2):163–72.
- [8] López-Gómez JJ, Pérez-Castrillón JL, García de Santos I, Pérez-Alonso M, Izaola-Jauregui O, Primo-Martín D, De Luis-Román DA. Influence of obesity on bone turnover markers and fracture risk in postmenopausal women. Nutrients 2022:14(8).
- [9] Lecka-Czernik B, Stechschulte LA, Czernik PJ, Dowling AR. High bone mass in adult mice with diet-induced obesity results from a combination of initial increase in bone mass followed by attenuation in bone formation; implications for high bone mass and decreased bone quality in obesity. Mol Cell Endocrinol 2015;410:35–41.
- [10] Ebeling PR, Nguyen HH, Aleksova J, Vincent AJ, Wong P, Milat F. Secondary osteoporosis. Endocr Rev 2022;43(2):240–313.
- [11] Cawthorn WP, Scheller EL. Editorial: bone marrow adipose tissue: formation, function, and impact on health and disease. Front Endocrinol (Lausanne) 2017;8:112.
- [12] Cornish J, Wang T, Lin JM. Role of marrow adipocytes in regulation of energy metabolism and bone homeostasis. Curr Osteoporos Rep 2018;16(2):116–22.
- [13] Tencerova M, Kassem M. The bone marrow-derived stromal cells: commitment and regulation of adipogenesis. Front Endocrinol 2016;7:127.
- [14] Wilson A, Trumpp A. Bone-marrow haematopoietic-stem-cell niches. Nat Rev Immunol 2006;6(2):93–106.
- [15] Wang LD, Wagers AJ. Dynamic niches in the origination and differentiation of haematopoietic stem cells. Nat Rev Mol Cell Biol 2011;12(10):643–55.
- [16] Pinho S, Frenette PS. Haematopoietic stem cell activity and interactions with the niche. Nat Rev Mol Cell Biol 2019;20(5):303–20.
- [17] Li J, Chen X, Lu L, Yu X. The relationship between bone marrow adipose tissue and bone metabolism in postmenopausal osteoporosis. Cytokine Growth Factor Rev 2020;52:88–98.
- [18] Lu X, Kong X, Wu H, Hao J, Li S, Gu Z, et al. UBE2M-mediated neddylation of TRIM21 regulates obesity-induced inflammation and metabolic disorders. Cell Metab 2023;35(8) (1390 405.e8).
- [19] Ambrosi TH, Scialdone A, Graja Á, Gohlke S, Jank AM, Bocian C, et al. Adipocyte accumulation in the bone marrow during obesity and aging impairs stem cellbased hematopoietic and bone regeneration. Cell Stem Cell 2017;20(6) (771 84 e6)
- [20] Pagnotti GM, Styner M, Uzer G, Patel VS, Wright LE, Ness KK, et al. Combating osteoporosis and obesity with exercise: leveraging cell mechanosensitivity. Nat Rev Endocrinol 2019;15(6):339–55.
- [21] Fantuzzi G. Adipose tissue, adipokines, and inflammation. J Allergy Clin Immunol 2005;115(5):911–9 (quiz 20).

- [22] Xue Y, Jiang L, Cheng Q, Chen H, Yu Y, Lin Y, et al. Adipokines in psoriatic arthritis patients: the correlations with osteoclast precursors and bone erosions. PLoS One 2012;7(10):e46740.
- [23] Neumann E, Junker S, Schett G, Frommer K, Muller-Ladner U. Adipokines in bone disease. Nat Rev Rheumatol 2016;12(5):296–302.
- [24] Zhang H, Wu X, Liang J, Kirberger M, Chen N. Irisin, an exercise-induced bioactive peptide beneficial for health promotion during aging process. Ageing Res Rev 2022;80:101680.
- [25] Xiong XQ, Geng Z, Zhou B, Zhang F, Han Y, Zhou YB, et al. FNDC5 attenuates adipose tissue inflammation and insulin resistance via AMPK-mediated macrophage polarization in obesity. Metab Clin Exp 2018;83:31–41.
- [26] Mazur-Bialy Al, Bilski J, Pochec E, Brzozowski T. New insight into the direct anti-inflammatory activity of a myokine irisin against proinflammatory activation of adipocytes. Implication for exercise in obesity. J Physiol Pharmacol 2017;68(2):243–51.
- [27] Liu TY, Shi CX, Gao R, Sun HJ, Xiong XQ, Ding L, et al. Irisin inhibits hepatic gluconeogenesis and increases glycogen synthesis via the PI3K/Akt pathway in type 2 diabetic mice and hepatocytes. Clin Sci (Lond) 2015;129(10):839–50.
- [28] Xiong XQ, Chen D, Sun HJ, Ding L, Wang JJ, Chen Q, et al. FNDC5 overexpression and irisin ameliorate glucose/lipid metabolic derangements and enhance lipolysis in obesity. Biochim Biophys Acta 2015;1852(9):1867–75.
- [29] Xue Y, Hu S, Chen C, He J, Sun J, Jin Y, et al. Myokine Irisin promotes osteogenesis by activating BMP/SMAD signaling via alphaV integrin and regulates bone mass in mice. Int J Biol Sci 2022;18(2):572–84.
- [30] Hu S, Xue Y, He J, Chen C, Sun J, Jin Y, et al. Irisin recouples osteogenesis and osteoclastogenesis to protect wear-particle-induced osteolysis by suppressing oxidative stress and RANKL production. Biomater Sci 2021;9(17):5791–801.
- [31] He X, Hua Y, Li Q, Zhu W, Pan Y, Yang Y, et al. FNDC5/irisin facilitates muscle-adipose-bone connectivity through ubiquitination-dependent activation of runt-related transcriptional factors RUNX1/2. J Biol Chem 2022;298 (3):101679.
- [32] Huang Y, Yin Y, Gu Y, Gu Q, Yang H, Zhou Z, et al. Characterization and immunogenicity of bone marrow-derived mesenchymal stem cells under osteoporotic conditions. Sci China Life Sci 2020;63(3):429–42.
- [33] Lin W, Gao J, Zhang H, Chen L, Qiu X, Huang Q, et al. Identification of molecular subtypes based on inflammatory response in lower-grade glioma. Inflamm Regen 2022;42(1):29.
- [34] Kim JM, Lin C, Stavre Z, Greenblatt MB, Shim JH. Osteoblast-osteoclast communication and bone homeostasis. Cells 2020;9:9.
- [35] Ali D, Tencerova M, Figeac F, Kassem M, Jafari A. The pathophysiology of osteoporosis in obesity and type 2 diabetes in aging women and men: the mechanisms and roles of increased bone marrow adiposity. Front Endocrinol (Lausanne) 2022;13:981487.
- [36] Perakakis N, Triantafyllou GA, Fernandez-Real JM, Huh JY, Park KH, Seufert J, et al. Physiology and role of irisin in glucose homeostasis. Nat Rev Endocrinol 2017;13(6):324–37.
- [37] Kim H, Wrann CD, Jedrychowski M, Vidoni S, Kitase Y, Nagano K, et al. Irisin mediates effects on bone and fat via alphaV integrin receptors. Cell 2018;175 (7) (1756 68 e17).
- [38] Chen N, Li Q, Liu J, Jia S. Irisin, an exercise-induced myokine as a metabolic regulator: an updated narrative review. Diabetes Metab Res Rev 2016;32 (1):51–9.
- [39] Aladag T, Mogulkoc R, Baltaci AK. Irisin and energy metabolism and the role of irisin on metabolic syndrome. Mini Rev Med Chem 2023;23(20):1942–58.
- [40] Kaneshiro S, Ebina K, Shi K, Higuchi C, Hirao M, Okamoto M, et al. IL-6 negatively regulates osteoblast differentiation through the SHP2/MEK2 and SHP2/Akt2 pathways in vitro. | Bone Miner Metab 2014;32(4):378–92.
- [41] Osta B, Benedetti G, Miossec P. Classical and paradoxical effects of TNF-alpha on bone homeostasis. Front Immunol 2014:5:48.
- [42] Forte YS, Renovato-Martins M, Barja-Fidalgo C. Cellular and molecular mechanisms associating obesity to bone loss. Cells 2023;12(4).
- [43] Sindhu S, Thomas R, Shihab P, Sriraman D, Behbehani K, Ahmad R. Obesity is a positive modulator of IL-6R and IL-6 expression in the subcutaneous adipose tissue: significance for metabolic inflammation. PLoS One 2015;10(7):e0133494.
- [44] Wang C, Tian L, Zhang K, Chen Y, Chen X, Xie Y, et al. Interleukin-6 gene knockout antagonizes high-fat-induced trabecular bone loss. J Mol Endocrinol 2016;57(3):161–70.
- [45] Li Y, Lu L, Xie Y, Chen X, Tian L, Liang Y, et al. Interleukin-6 knockout inhibits senescence of bone mesenchymal stem cells in high-fat diet-induced bone loss. Front Endocrinol 2020;11:622950.
- [46] Bai J, Wang Y, Wang J, Zhai J, He F, Zhu G. Irradiation-induced senescence of bone marrow mesenchymal stem cells aggravates osteogenic differentiation dysfunction via paracrine signaling. Am J Phys Cell Phys 2020;318(5): C1005–17.
- [47] He X, Hu W, Zhang Y, Chen M, Ding Y, Yang H, et al. Cellular senescence in skeletal disease: mechanisms and treatment. Cell Mol Biol Lett 2023;28(1):88.
- [48] Liu S, Cui F, Ning K, Wang Z, Fu P, Wang D, et al. Role of irisin in physiology and pathology. Front Endocrinol 2022;13:962968.
 [49] Waseem R, Shamsi A, Mohammad T, Hassan MI, Kazim SN, Chaudhary AA,
- [49] Waseem R, Shamsi A, Mohammad T, Hassan MI, Kazim SN, Chaudhary AA, et al. FNDC5/Irisin: physiology and pathophysiology. Molecules (Basel Switzerland) 2022;27(3).
- [50] Ma EB, Sahar NE, Jeong M, Huh JY. Irisin exerts inhibitory effect on adipogenesis through regulation of wnt signaling. Front Physiol 2019;10:1085.
- [51] Qiao X, Nie Y, Ma Y, Chen Y, Cheng R, Yin W, et al. Irisin promotes osteoblast proliferation and differentiation via activating the MAP kinase signaling pathways. Sci Rep 2016;6:18732.

- [52] Ma Y, Qiao X, Zeng R, Cheng R, Zhang J, Luo Y, et al. Irisin promotes proliferation but inhibits differentiation in osteoclast precursor cells. FASEB J 2018 (fj201700983RR).
- [53] Estell EG, Le PT, Vegting Y, Kim H, Wrann C, Bouxsein ML, et al. Irisin directly stimulates osteoclastogenesis and bone resorption in vitro and in vivo. Elife 2020:9.
- [54] Franchini M, Monnais E, Seboek D, Radimerski T, Zini E, Kaufmann K, et al. Insulin resistance and increased lipolysis in bone marrow derived adipocytes stimulated with agonists of Toll-like receptors. Horm Metab Res 2010;42 (10):703–9.
- [55] Yu Q, Li G, Ding Q, Tao L, Li J, Sun L, et al. Irisin protects brain against ischemia/ reperfusion injury through suppressing TLR4/MyD88 pathway. Cerebrovasc Dis 2020;49(4):346–54.
- [56] Slate-Romano JJ, Yano N, Zhao TC. Irisin reduces inflammatory signaling pathways in inflammation-mediated metabolic syndrome. Mol Cell Endocrinol 2022;552:111676.
- [57] Li Q, Zhang M, Zhao Y, Dong M. Irisin protects against LPS-stressed cardiac damage through inhibiting inflammation, apoptosis, and pyroptosis. Shock 2021;56(6):1009–18.
- [58] Shaw A, Tóth BB, Király R, Arianti R, Csomós I, Póliska S, et al. Irisin stimulates the release of CXCL1 From differentiating human subcutaneous and deep-neck

- derived adipocytes via upregulation of NF κ B pathway. Front Cell Dev Biol 2021:9:737872.
- [59] Zhang YW, Cao MM, Li YJ, Lu PP, Dai GC, Zhang M, et al. Fecal microbiota transplantation ameliorates bone loss in mice with ovariectomy-induced osteoporosis via modulating gut microbiota and metabolic function. J Orthop Translat 2022:37:46–60.
- [60] Zhang YW, Wu Y, Liu XF, Chen X, Su JC. Targeting the gut microbiota-related metabolites for osteoporosis: the inextricable connection of gut-bone axis. Ageing Res Rev 2024;94:102196.
- [61] Zhang YW, Cao MM, Li YJ, Dai GC, Lu PP, Zhang M, et al. The regulative effect and repercussion of probiotics and prebiotics on osteoporosis: involvement of brain-gut-bone axis. Crit Rev Food Sci Nutr 2023;63(25):7510–28.
- [62] Zhang YW, Song PR, Wang SC, Liu H, Shi ZM, Su JC. Diets intervene osteoporosis via gut-bone axis. Gut Microbes 2024;16(1):2295432.
- [63] Kim H, Wrann CD, Jedrychowski M, Vidoni S, Kitase Y, Nagano K, et al. Irisin mediates effects on bone and fat via αν integrin receptors. Cell 2018;175(7) (1756 68.e17).
- [64] Maak S, Norheim F, Drevon CA, Erickson HP. Progress and challenges in the biology of FNDC5 and irisin. Endocr Rev 2021;42(4):436–56.